Proceedings of Turbomachinery Technical Conference and Exposition
ASME 2018 TurboExpo
June 11-15, 2018, Oslo, Norway

GT2018-76214

EFFECT OF THE GAS TO WALL TEMPERATURE RATIO ON THE BYPASS TRANSITION

Riccardo Rubini* **Roberto Maffulli†** **Tony Arts‡**

Department of Turbomachinery and Propulsion
von Karman Institute
Rhode Saint Genese, Belgium 1640

ABSTRACT

The study of boundary layer transition plays a fundamental role in the field of turbomachinery owing to its strong influence on skin friction and heat transfer. The understanding of the laminar to turbulent transition can help designers to improve the aerodynamic and thermodynamic performances both of the components and of the whole machine. Transition models are nowadays commonly used tools in both research and design practice. In the context of high-pressure turbines design, it is then of particular interest to understand if such models are able to predict the effect of temperature on bypass transition and, in case of positive answer, the reasons of their behaviour. This becomes even more interesting as the effect of the flow aero-thermal coupling becomes prominent in the analysis of such phenomena, as this effect is typically not accounted for in the validation of turbulence models. Two state-of-the-art transition models are examined in the present contribution: the $\gamma - Re_\theta$ model developed by Langtry and Menter [1] and the $k - k_l - \omega$ model by Walters and Cokljat [2]. The two models have been chosen as they use two radically different approaches to describe the transition process: an empirical, correlation-based one for the former opposed to a phenomenological, based on local transport, for the latter. To isolate the effects of the temperature ratio on the transition, the simulations have been performed keeping the same values of Reynolds and Mach numbers and changing the value of the wall to freestream Temperature Ratio (TR). The results of the two transition models have been compared between them, as well as with experimental results obtained as part of a parallel effort, showing how a transition modelling based on local transport, rather than empirical correlations should be favou.

NOMENCLATURE

α_t Turbulent thermal diffusivity
BC Boundary Conditions
BP Bypass Transition
CFD Computational Fluid Dynamics
γ Heat capacity ratio for perfect gas
δ Local boundary layer thickness
DNS Direct Numerical Simulation
FSTI Free Stream Turbulence Intensity
FV Finite Volume
HTC Heat Transfer Coefficient
LE Leading Edge
LES Large Eddy Simulation
LST Linear Stability Theory
M_{is} Isentropic Mach number
NAT Natural Transition
$p_{0_{in}}$ Inlet Total Pressure
p Static Pressure
PS Pressure Side
q_w Wall Heat Flux
RANS Reynolds Averaged Navier Stokes
SS Suction Side

*Currently PhD student at Southampton University. E-mail: r.rubini@soton.ac.uk.
†Currently Research Assistant at Oxford University. E-mail: roberto.maffulli@eng.ox.ac.uk.
‡Email: arts@vki.ac.be

Copyright © 2018 by ASME

SST Shear Stress Tensor
T_w Wall Temperature
$T_{0_{in}}$ Inlet Total Temperature
TE Trailing Edge
TR Temperature Ratio ($T_{0_{in}}/T_w$)
U Velocity Magnitude
Ω Vorticity Magnitude
k_t Turbulent Kinetic Energy
k_l Laminar Kinetic Energy
ω Specific dissipation ratio
ν Kinematic Viscosity
γ Perfect Gas Constant ($\frac{c_p}{c_v}$)
Re_θ Reynolds Number based on the momentum thickness
Re_{θ_c} Critical Reynolds Number based on the momentum thickness
Tu Turbulence Intensity ($\frac{\sqrt{2/3k}}{U}$)
L_t Integral Length Scale
Re_{is} Isentropic Reynolds Number
Re_v Reynolds Number based on the vorticity $\frac{y^2\Omega}{\nu}$
Pr_t Turbulent Prandtl Number $\frac{\nu_T}{\alpha_T}$
y Wall normal coordinate

1 INTRODUCTION

Laminar to turbulent transition plays a central role in the performance of modern gas turbines, affecting both aerodynamic and thermal performance of the machine [3]. Due to its importance, correct numerical prediction of transition is paramount for turbomachinery design. However, current modelling tools are still recognized to be the source of major uncertainty in flow predictions [4].

Particularly, in a typical high-speed turbomachinery flow, a strong coupling exists between the aerodynamic and thermal field [5], [6]. Given the presence of this interaction, and the importance of transition modelling in turbine flows, an investigation of the sensitivity of modern transition models on thermal boundary conditions becomes of particular interest.

When it comes to analyse the influence of the thermal field on transition, a distinction should be made with respect to the transition mechanism of interest. The issue has been discussed by several authors in the context of linear stability theory (*LST*) for natural transition, but to a lesser extent for other transition mechanisms.

A work from Ozgen [7], proposes to modify the incompressible Navier-Stokes system in order to account for the dependency of the thermo-physical properties of the fluid with the temperature. As result he found out that for variable density flows, heating continuously destabilizes the boundary layer, observing an opposite effect for constant density flows. The author ascribed those effects to the modification of the integral boundary layer parameters as well as the different evolution of the fluid's thermodynamic properties.

A similar analysis has been performed by Shafer and Severin [8] who found out how the stability of the boundary layer is influenced in different ways according to the direction of the heat flux. The physical explanation lays in the conjoint effect of the variation of viscosity and density into the lower part of the boundary layer. A similar description was given by Harrison et al. [9] when considering boundary layer heating under favourable pressure gradient.

Given the magnitude of the external disturbances, natural transition is rarely found in high pressure turbines, with by-pass transition being the dominant mechanism. The effect of aerothermal coupling on by-pass transition is less understood and less literature has been devoted to the general understanding of the issue.

In his experimental work, Sharma [10] observed how the value of the turbulent Prandtl number Pr_t may present some kind of functional dependency with respect to the value of the free-stream pressure gradient. Most importantly, the author established a connection between the transitional thermal boundary layer and the momentum boundary layer for by-pass transition. A key conclusion of the study was to realize how the assumption, typical of RANS modelling, of invariable turbulent Prandtl number may result in wrong predictions in the presence of coupling between thermal and momentum boundary layers.

Sohn et al. [11] attempted to characterize the bypass transition in a heated boundary layer. The result was the observation of an increase of the heat transfer due probably to the enhancement of low frequencies modes. A similar study was carried on by Ferreira and Arts [12] on a high pressure turbine cascade. The main idea was to measure the heat flux along the blade surface and, from the time trace of the signal, reconstruct the intermittency function of the boundary layer characterizing then the transition process. The results of the study were not conclusive, however, due to the restricted range of conditions analysed.

In a recent study, Arnal and Vermeersch [13] using optimal growth theory, seem to show how cooling the surface has destabilizing effects on the boundary layer for higher subsonic values of the Mach number and almost negligible effects for supersonic ones. This effect of cooling in promoting boundary layer transition has been observed experimentally by Back et al. [14] and is also consistent with the destabilizing effect of cooling on bypass transition described by Reshotko and Tumin [15].

The relevant literature indicates the existence of a clear aerothermal coupling in a typical high speed turbomachinery flow. This, together with the importance of transition and its dependence on local boundary layer characteristics, constitutes the basis of the present work. It becomes thus relevant to understand, for modern transition models:

- to what extent they are affected by the thermal boundary conditions,
- whether numerical predictions in this respect can be consid-

Copyright © 2018 by ASME

ered to be in line with experimental results,
- how much a typical correlation-based approach for transition modelling can be considered reliable in the presence of strong aero-thermal coupling in the flow.

2 WORKING PRINCIPLES OF THE RANS TRANSITION MODELS CONSIDERED IN THIS STUDY

A brief overview of the two RANS transition models used in this work is given in the following sections. A deep explanation of the models and their equations is outside the scope of this work. The description given here is aimed at highlighting the two different philosophies on which the models rely. The reader is referred to the original work by the respective authors of the models for a complete description of their working principles.

The $k-k_l-\omega$ transition model [2] is based on the observation that bypass transition is promoted by streamwise flow oscillations having a different behaviour than turbulent fluctuations. Mayle [16] first proposed to model these fluctuations through the definition of a laminar kinetic energy k_l. In the $k-k_l-\omega$ model, a transport equation for k_l is solved together with the equations for k and ω. The model marks the onset of transition when the ratio between the turbulent production time-scale and the molecular diffusion time-scale exceeds a defined value. Transition is modelled through a transfer of laminar kinetic energy to turbulent kinetic energy. The advantage of this method is that the turbulence closure does not need empirical input.

The $\gamma-Re_\theta$ model [17] is, differently from the $k-k_l-\omega$, a correlation based model. The model is based on the SST formulation of $k-\omega$ turbulence model, but solves two extra equations: one for the intermittency (γ) and the second for the Reynolds number based on the transition onset momentum thickness (Re_θ). The intermittency is used to trigger the production of turbulent kinetic energy in the boundary layer, while Re_θ is needed to mark the start of the transition. The model uses a correlation that provides the value of the transition Re_θ outside of the boundary layer, as function of the external flow conditions (Tu and pressure gradient). This value is then diffused in the boundary layer using a transport equation for Re_θ. In the intermittency equation, the ratio between local values of momentum thickness Re_θ and the critical transition Re_{θ_c} (provided by another correlation) is used to mark the inception of transition.

As shown, the two models rely on two markedly different approaches with the $\gamma-Re_\theta$ using a correlation linking the freestream conditions to the boundary layer transition Re_θ. As will be shown in the following, this difference results in an inconsistent behaviour of the $\gamma-Re_\theta$ model when the same TR is obtained by altering freestream conditions rather than wall temperature.

3 NUMERICAL METHODOLOGY

The analyses presented in the following sections have been performed on a steady 2D flow around the VKI-LS89 nozzle guide vane [18]. The geometry used is shown in Fig. 1. Symmetry boundary conditions have been used on the two planes normal to the spanwise direction.

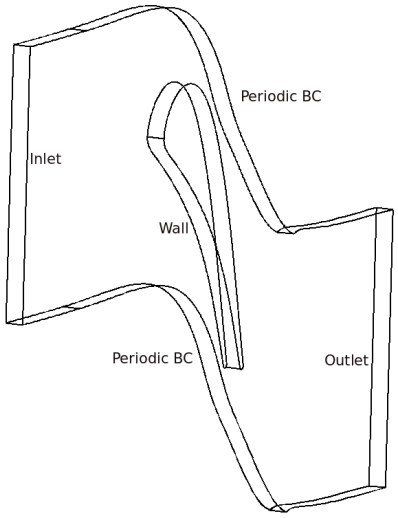

FIGURE 1: Computational domain used in the present contribution

Two solvers have been adopted for the analysis. The simulations done using γ-Re_θ have been performed using Numeca Fine Turbo. The pressure-based solver of ANSYS Fluent has been used for the k-k_l-ω simulations. Both solvers used second order spatial discretization. The reason for the choice of the two solvers was due to the fact that k-k_l-ω was only available on Fluent.

NUMECA-Autogrid has been used to generate the computational grid. The computational domain has been discretised through a multi-block hexahedral mesh using an O-grid block around the blade surrounded by four H-grid domains. The inlet has been located one chord upstream the leading edge and the outlet at 1.5 chords downstream in order to limit as much as possible the influence of the domain boundaries on the solution. The extension of the domain in the spanwise direction was chosen as 10% of the axial chord, enough to reduce the effects of the endwalls. In order to correctly model the effects of temperature, air has been treated as a perfect gas with viscosity varying with temperature according to Sutherland's law. Dependence of thermal conductivity on temperature has been modelled as well.

4 GRID INDEPENDENCE AND VALIDATION

Grid independence is a crucial aspect in order to guarantee the reliability of the results, specially as transition models seem to suffer from a higher sensitivity than conventional turbulence models.

Given that two different solvers, and two different transition models, have been used during the analysis, two separate grid independence studies have been carried out. During the grid

Copyright © 2018 by ASME

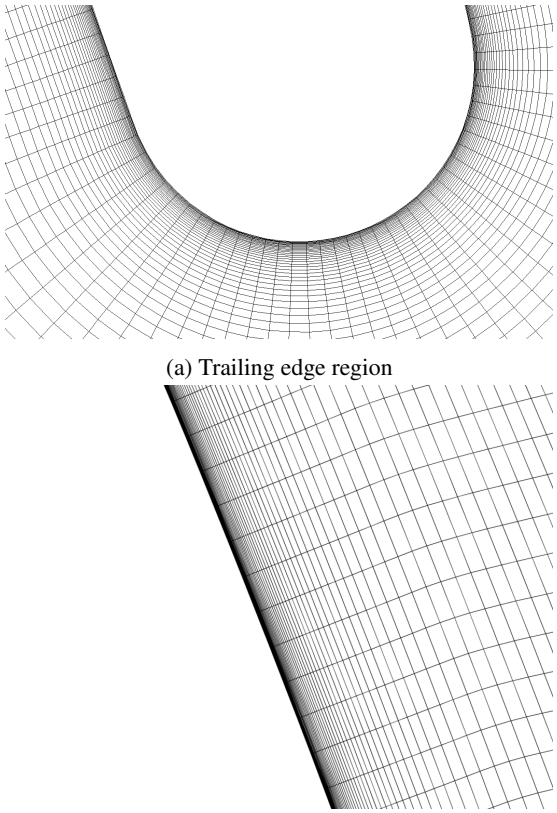

(a) Trailing edge region

(b) Suction side boundary layer region

FIGURE 2: Details of the used computational grid

sensitivity study we have considered four different meshes respectively with $50 \cdot 10^3$, $80 \cdot 10^3$,$120 \cdot 10^3$ and $200 \cdot 10^3$ cells. In both cases the mesh density has been altered both in the streamwise and spanwise directions. Particular attention has been given to limit the grid expansion ratio from the wall to 1.1. In order to properly resolve the boundary layer, a fixed wall distance of about 10^{-5} meters has been imposed for all considered grids. This allowed to have $y+ < 1$ along the whole blade surface to ensure a low Reynolds approach. Proper control of the grid quality in the boundary layer region has been assured by using an O-grid block around the blade. Details of the used grid in the boundary layer and trailing edge regions are shown in Fig. 2.

The sensitivity analysis has been performed on the value of the Heat Transfer Coefficient (HTC) defined as:

$$HTC = \frac{q_w}{T_w - T_{0_{in}}}, \tag{1}$$

where q_w is the wall heat flux, T_w the wall temperature and $T_{0_{in}}$ the inlet total temperature. The pressure distribution has been found to be quite insensitive to grid node count, at least on the level of density tried in the present study.

Grid independence was considered to be reached when an

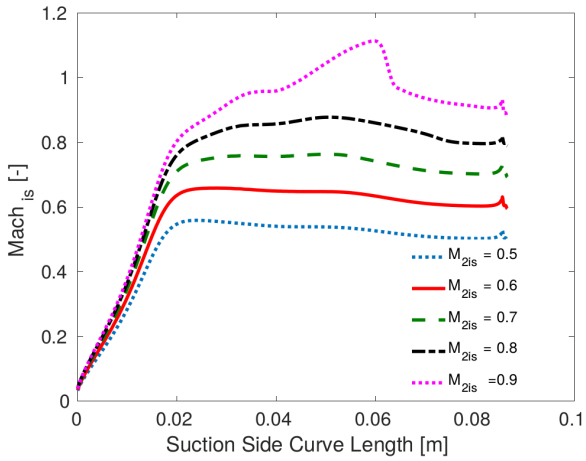

FIGURE 3: M_{is} distribution on the suction side at various downstream $M_{2_{is}}$.

increase of node count would not alter the transition point nor the general heat transfer levels. The computed HTC distributions have been compared with the experimental results by Arts [19]. A further aerodynamic validation has been performed on the value of the isentropic Mach number.

Grid independence has been reached, for both models, on a grid of about $120 \cdot 10^5$ nodes that has been used for the remaining part of this work.

5 PRELIMINARY AERODYNAMIC STUDY

It is known from literature [19] that the transition location is mainly influenced by three parameters: free-stream turbulence intensity (FSTI), free-stream pressure gradient and Reynolds number. Other parameters such as wall temperature and roughness are considered to have a lower order impact on transition. Therefore, in order to observe the effect of the temperature on the transition we have to exclude the influence of the three main drivers as much as possible. A parametric study on the aerodynamic behaviour of the suction side flow has been performed at various back pressure levels, with constant levels of FSTI and Reynolds number. This was done to find an operating condition where the suction side pressure distribution would be as flat as possible. Limiting the pressure gradients was important to isolate the effect of the temperature ratio and ensure that transition would not be triggered by a strong pressure gradient.

To perform this analysis five simulations have been performed at different value of the isentropic Mach number (defined in Eq. (2)) ranging from 0.5 to 0.9.

$$M_{2is} = \sqrt{\left[\left(\frac{p_{0_{in}}}{p}\right)^{\frac{\gamma}{\gamma-1}} - 1\right]\frac{2}{\gamma-1}} \tag{2}$$

Copyright © 2018 by ASME

For too high exit Mach numbers, Fig. 3 shows how the velocity distribution shows pressure gradients in the rear part of the blade that could outweigh the effect of the temperature. On the other hand in the case of too high back pressure, the M_{is} levels decrease to too low values. Finally an operation condition with an exit isentropic Mach number of 0.55 has been chosen for the experimental campaign.

6 AERO-THERMAL ANALYSIS OF TEMPERATURE RATIO EFFECT ON TRANSITION

The main results of this work will be presented in the present section. Two simulation campaigns with the two different transition models have been conducted on the LS89 profile [19]. The distributions of HTC (as defined in Eq. (1)) as well as detailed boundary layer traversing data have been analyzed under varying freestream to wall Temperature Ratio (TR). The latter has been defined as:

$$TR = \frac{T_{0_{in}}}{T_w}, \tag{3}$$

where $T_{0_{in}}$ is the freestream inlet total temperature and T_w the wall temperature.

Before introducing the results, which will be presented separately for the two transition models, it is important to draw a distinction on how the data have been obtained for experiments and numerical simulations.

Experiments have been carried out in a short duration facility using an uncooled blade profile. The impossibility to cool the blade wall meant that the only way to alter the TR in experiments was to modify the inlet total temperature, while inlet/outlet boundary conditions were modified accordingly to keep constant the exit Reynolds and Mach numbers. These working conditions will be referred to as constant T_w. The TR can also be modified by keeping constant the freestream conditions and changing the wall temperature. This approach — referred to as *constant* $T_{0_{in}}$ — has been used in the numerical simulations only, therefore there are no experimental results for these working conditions. The authors would like to point out that, despite all non-dimensional parameters being matched between a constant freestream and a constant wall temperature case with the same TR, the two cases are not comparable due to the inherent difference in how the TR is achieved and given the working principles of the used transition models. Since experimental data have been gathered under constant T_w, comparison between CFD and experiments will only be limited to those conditions.

The use of both approaches was needed to reach the deepest possible insight about the behaviour of the models and to test their internal consistency. Given its nature of a correlation-based model where transition is linked to freestream conditions, it is expected that the $\gamma - Re_\theta$ would be particularly sensitive to their variation. For this turbulence model, accurate results will be reported for both constant T_w and constant $T_{0_{in}}$ conditions in separate sections. The results obtained using the $k - k_l - \omega$ model, instead, have been grouped under a single section (Sec. 6.4) for the sake of brevity as the models showed a very consistent behavior under both constant $T_{0_{in}}$ and constant T_w.

$T_{wall}[K]$	M_{2is}	Re_{2is}	Tu	$L_t[m]$	TR
294	0.55	$9.5 \cdot 10^5$	0.8	0.02	1.1-1.3-1.5

TABLE 1: Aero-thermal conditions used for constant T_w calculations and for experiments.

$T_0[K]$	M_{2is}	Re_{2is}	Tu	$L_t[m]$	TR
441	0.55	$9.5 \cdot 10^5$	0.8	0.02	1.1-1.3-1.5

TABLE 2: Aero-thermal conditions used for constant $T_{0_{in}}$ calculations.

Section	1	2	3	4	5	6
Location % of SS	6	23	47	58	70	82

TABLE 3: Locations, in percentage of the suction side curve length, of the traversing slices.

Both experiments and simulations have been performed imposing the following boundary conditions:

- Inlet total pressure and temperature
- Outlet static pressure
- Constant wall temperature on the blade profile

All boundary conditions above were varied from case to case to match the required $Re_{2_{is}}$, $M_{2_{is}}$ and TR. The reference aero-thermal conditions used for CFD calculations and experiments for both *constant* T_w and *constant* $T_{0_{in}}$ conditions are detailed in Tabs. 1 and 2.

A fine tuning of the inlet turbulent boundary conditions has been performed in order to match the measured data from the wind tunnel turbulence characterization performed by Fontaneto [20].

The data presented in what follows have been obtained considering a 1% FSTI. This ensures, under the considered profile operating conditions that boundary layer transition happens at around 50% of the suction side length, where the velocity profile is mostly flat.

Boundary layer traversing has been performed at different locations along the suction side in order to investigate the evolution of the relevant flow parameters under different temperature ratio conditions. The locations of the traversing slices are shown in Fig. 4 and their detailed positions listed in Tab. 3.

Copyright © 2018 by ASME

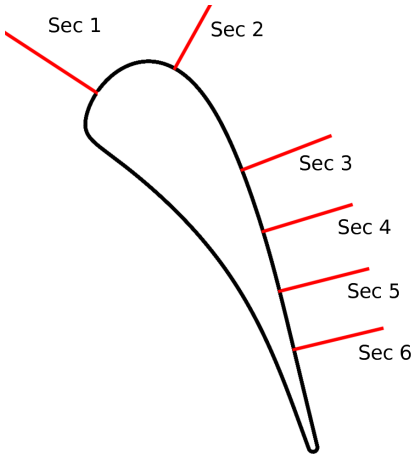

FIGURE 4: Location of the boundary layer traversing cuts along the suction side

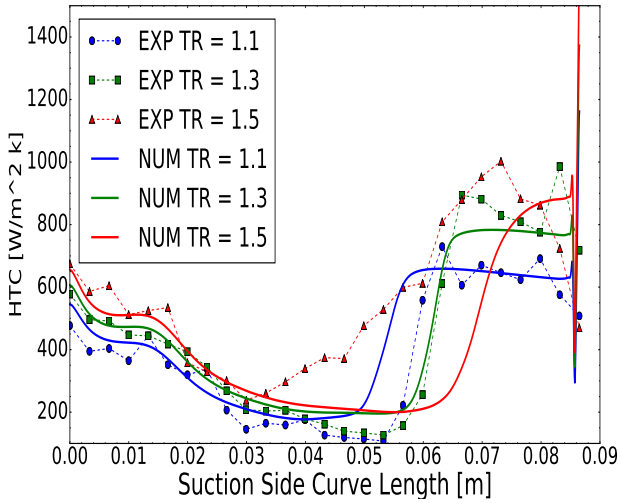

FIGURE 5: Blade HTC distribution at different TR obtained at constant T_w: comparison between experiments and CFD (obtained using $\gamma - Re_\theta$ model).

6.1 $\gamma - Re_\theta$ model with constant T_w

The first set of simulations has been performed with the $\gamma - Re_\theta$ model under varying freestream temperature. The obtained HTC distribution is reported in Fig. 5.

The model seems to capture an effect of the TR on transition: unfortunately the trend is the opposite with respect to the one shown by experimental results. The increase of temperature ratio seems to retard the transition instead of anticipating it as shown from the experiments.

In order to better understand the reason for this observed behaviour of the model, the values of the more relevant kinematic, turbulent and physical quantities have been investigated in the location of the boundary layer traversing slices. The results are

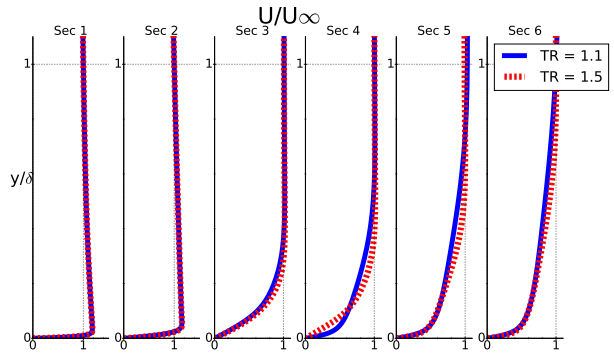

FIGURE 6: Distribution of velocity magnitude among the boundary layer traversing locations. $\gamma - Re_\theta$ model, constant T_w.

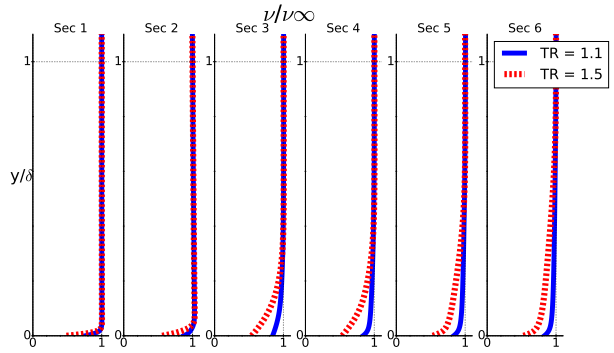

FIGURE 7: Distribution of kinematic viscosity among the boundary layer traversing locations. $\gamma - Re_\theta$ model, constant T_w.

summarized in Figs. 6 to 9. In those figures, the ordinate represents the distance from the wall y divided by the value of the local thickness of the boundary layer δ. The abscissa is the value of the analysed quantities, divided with the respective freestream value in the case of a dimensional variable.

Velocity: From Fig. 6 it is easy to observe how the compressibility effects that strongly couple the kinematic and thermal field cause some differences in the shape of the velocity profile already in the laminar part: sections 1, 2 and 3. In section 4 the profile shape changes because of the anticipated transition in the lower TR case. The different evolution of transition influences the downstream velocity profiles as well, as shown in sections 5 and 6.

Kinematic viscosity: One of the variables that triggers the onset of the transition is the local vorticity Reynolds number defined as $Re_v = \frac{y^2\Omega}{\nu}$. Both the density and the dynamic viscosity are temperature dependent. It is then interesting to see what is the evolution of the kinematic viscosity as this can have potential effects on the transition criteria.

Copyright © 2018 by ASME

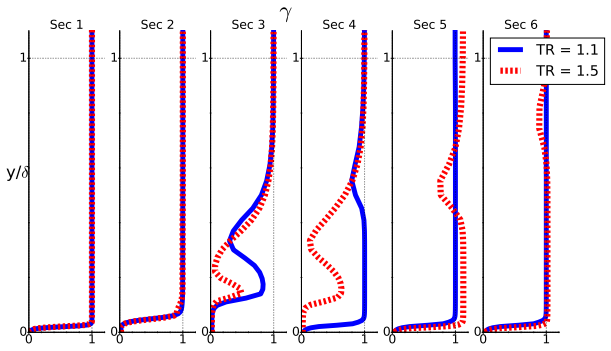

FIGURE 8: Distribution of intermittency among the boundary layer traversing locations. $\gamma - Re_\theta$ model, constant T_w.

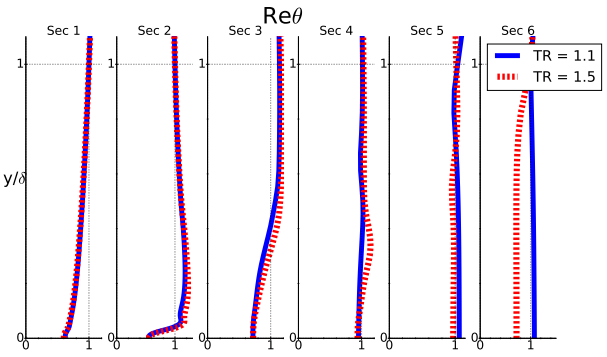

FIGURE 9: Distribution of momentum thickness Reynolds number Re_θ among the boundary layer traversing locations. $\gamma - Re_\theta$ model, constant T_w.

As the temperature grows, the dynamic viscosity increases according to the Sutherland's law, while the density decreases following the perfect gas law. As proposed by Schafer et al. [8] in the study of the natural transition, due to the opposite effect of the variation of density and viscosity, it is more convenient to study the stability in terms of the kinematic viscosity defined as the ratio of the two quantities $\nu = \frac{\mu}{\rho}$. From Fig. 7 it is possible to see how the combined effect of the decrease of viscosity and increase of density, produces a appreciable variation of kinematic viscosity near the wall. This effect must be taken into consideration because of the dependency of Re_v [17] on the value of this parameter.

Turbulent quantities: The last quantities that have been considered in the analysis are the variables transported in the transition model.

From the distribution of the intermittency (Fig. 8), it is possible to understand the state of the boundary layer. In particular we can see how the flow is largely laminar in the first two sections where γ is zero for the whole thickness of the boundary layer (very thin in these sections). In the third section, transition takes place for the lower TR, this can be seen thanks to the distribution of γ that grows progressively from zero to one inside the boundary layer itself. Finally the last two cuts show a fully turbulent boundary layer in both cases, with values of intermittency different from one only in the viscous sublayer.

The distribution of the Reynolds number based on the momentum thickness across the different cuts is shown in Fig. 9. Differences can be observed along the whole extent of the boundary layer. The results suggest that those differences, together with the effect of the freestream conditions on the critical Reynolds number Re_{θ_c} play a critical role on the effect of TR on transition for this model.

6.2 $\gamma - Re_\theta$ model with constant $T_{0_{in}}$

Given the dependence of the $\gamma - Re_\theta$ model on freestream conditions, and given that one would expect the TR as a non-dimensional parameter to determine the HTC [21, 22], disregarding on how this TR has been obtained, it becomes relevant to investigate what results can be obtained with the $\gamma - Re_\theta$ if freestream conditions are fixed.

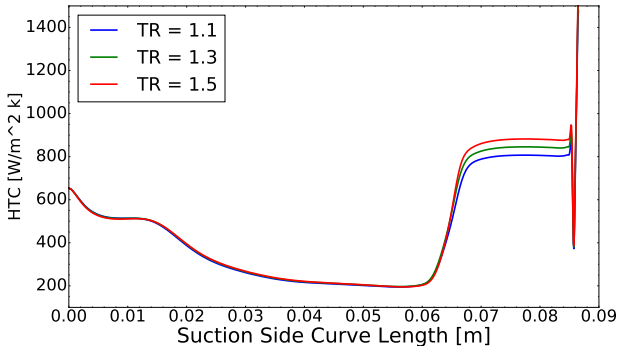

FIGURE 10: Blade HTC distribution at different TR obtained at constant $T_{0_{in}}$. No evident effect of the temperature ratio on the transition location.

The distribution of blade HTC (Fig. 10) shows that the model does not show the same behaviour as for the constant T_w cases. While a strong effect was shown in the previous case, for the present conditions very negligible influence of TR is seen.

Velocity: The velocity profiles inside the boundary layer traversing sections are shown in Fig. 11. Differently from what seen for the case with constant T_w, no appreciable differences are seen for this case. This is consistent with the observation that no marked alteration in the transition behavior is observed under the considered conditions.

Kinematic viscosity: Figure 12 shows the evolution of the kinematic viscosity across the six traversing locations on the suction side. A general evolution similar to what observed for the

Copyright © 2018 by ASME

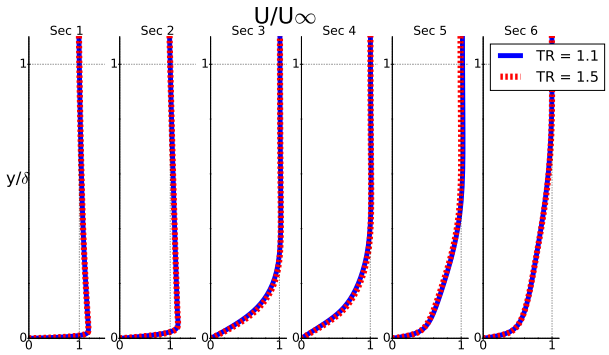

FIGURE 11: Distribution of velocity magnitude across the boundary layer traversing locations. $\gamma - Re_\theta$ model, constant $T_{0_{in}}$.

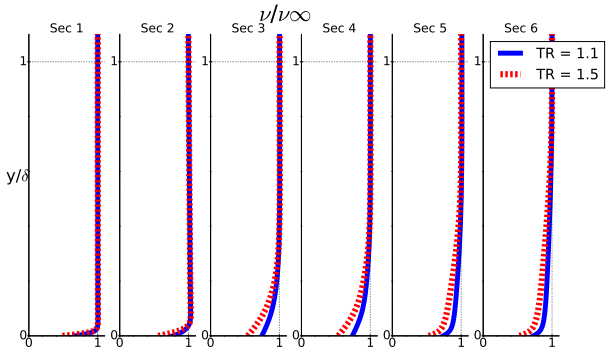

FIGURE 12: Distribution of kinematic viscosity across the boundary layer traversing locations. $\gamma - Re_\theta$ model, constant $T_{0_{in}}$.

constant T_w case can be seen, though smaller differences are observed between the two TR cases at various traversing locations compared with the constant T_w case (see Fig. 7).

It is interesting to notice how the influence of the temperature on the density and viscosity is propagated inside the boundary layer from the first section to the final one. This behaviour could have some interesting effects on the development of the turbulent kinetic energy. It has been observed — the results not being shown here for the sake of brevity — that, despite the transition took place in the same location, the turbulent kinetic energy evolves in a quite different way along the blade, this could be due to different values of density and viscosity as velocity gradients are largely unchanged for the present case.

Turbulent quantities: As done previously, the turbulent quantities that have been examined are the intermittency and momentum thickness Reynolds number.

Regarding the intermittency (Fig. 13) no major differences in its evolution can be found. This was to be expected given the

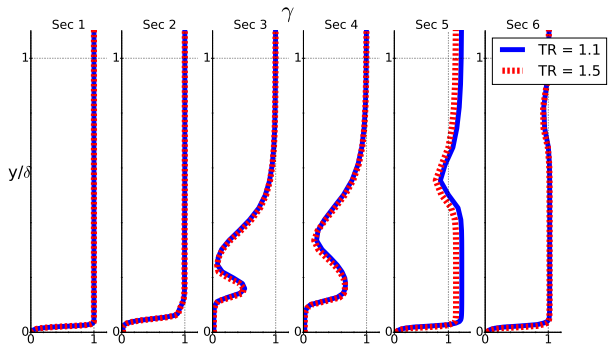

FIGURE 13: Distribution of intermittency across the boundary layer traversing locations. $\gamma - Re_\theta$ model, constant $T_{0_{in}}$.

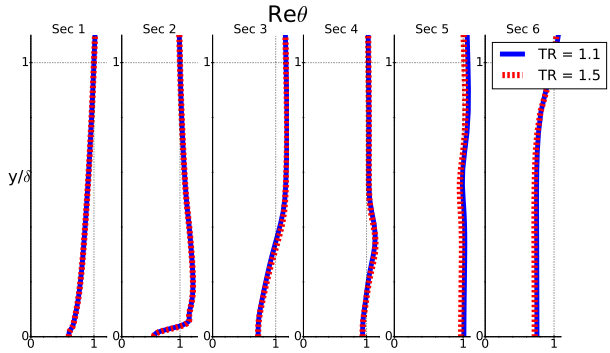

FIGURE 14: Distribution of momentum thickness Reynolds number Re_θ across the boundary layer traversing locations. $\gamma - Re_\theta$ model, constant $T_{0_{in}}$.

negligible effect of TR on the transition point for the examined conditions.

Also the distribution of the momentum thickness Reynolds number does not show marked differences between the two different temperature ratios. A comparison with the results of Fig. 9 seems to suggest that the value of Re_θ is strongly affected by the freestream conditions than by the wall temperature itself.

6.3 $\gamma - Re_\theta$ concluding remarks

Given the observed behaviour of the model, it is possible to conclude that the $\gamma - Re_\theta$ model is not able to capture, even qualitatively, the experimental results. In particular it has been found that:

- for the case at constant wall temperature the model predicts a stabilization of the flow when increasing the temperature ratio while the experiments show the opposite,
- for the case at constant freestream conditions the model does not show any dependence on the TR.

This behaviour can be explained analysing the mechanism triggering the transition in the model. In what follows the same

Copyright © 2018 by ASME

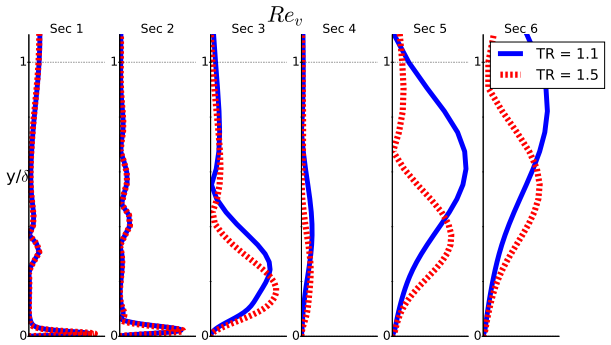

FIGURE 15: Distribution of vorticity Reynolds number Re_v across the boundary layer traversing locations. $\gamma - Re_\theta$ model, constant T_w.

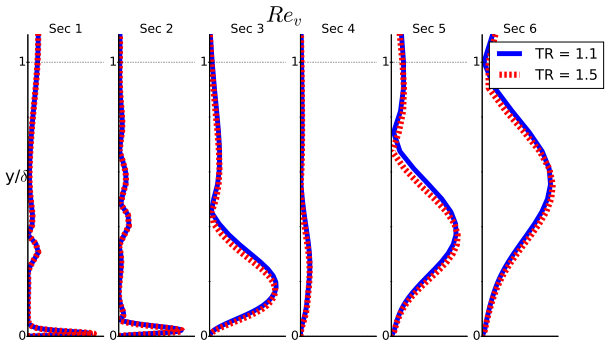

FIGURE 16: Distribution of vorticity Reynolds number Re_v across the boundary layer traversing locations. $\gamma - Re_\theta$ model, constant $T_{0_{in}}$.

symbols used in the original formulation of the model [17] will be used without giving more details than necessary on their meaning in order not to over-complicate the text. The reader is referred to the original paper for detailed explanation on the working principles of the model.

Production of intermittency due to transition for the $\gamma - Re_\theta$ is promoted by an increase of the ratio $\frac{Re_v}{Re_{\theta_c}}$ and/or a decrease of $R_T = \frac{\rho k}{\mu \omega}$. Thus, the parameters that drive transition are the turbulent kinetic energy and dissipation, the kinematic viscosity ν — contained also in the vorticity Reynolds number Re_v — and the value of the transition onset Reynolds number Re_{θ_c}. The value of the latter is related to the value of the transported scalar Re_θ through a proprietary correlation. Local values of Re_θ are the result of the diffusion in the boundary layer of the freestream values, coming from an empirical correlation. Different developments of k and ω due to the different temperature field may play a role but this has been found to be secondary, at least in the present study. Given this, the behaviour of the two different cases can be justified as follows:

- For the simulations at constant wall temperature, the increase of TR causes a reduction in the pre-transitional values of Re_θ (see Fig. 9). The different freestream temperature causes a considerable alteration in the distribution of Re_v (see Fig. 15). The combined effect of the two suppresses the production of intermittency inside the boundary layer and retards transition for the high temperature ratio case.
- For the case at constant freestream temperature, instead, the model seems to be largely insensitive to variations in TR. Both the Re_θ (Fig. 16) and Re_v (Fig. 14) distributions in the boundary layer traversing sections are only marginally affected by the TR. As a result production of intermittency is not influenced by the wall thermal boundary condition and the transition point is unchanged.

The behaviour of the model seems to be strongly related to the evolution of the Re_θ in the freestream as well as to the sensitivity of the correlation to determine Re_{θ_c} to freestream variations. This appears to limit the consistency of the model when TR effects are of concern. Different behaviours — both qualitatively and quantitatively — have been in fact observed when acting on freestream or wall conditions and still preserving the relevant non-dimensional similitude parameters.

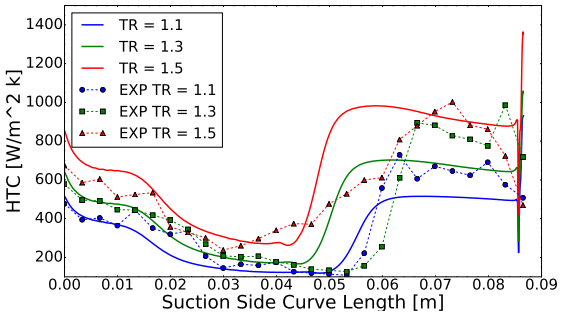

FIGURE 17: Blade HTC distribution at different TR obtained at constant T_w: comparison between experiments and CFD (obtained using $k - k_l - \omega$ model).

6.4 $k - k_l - \omega$ model

Figures 17 and 18 show the results for constant T_w and constant $T_{0_{in}}$ respectively. It is important to stress out that in the case of Fig. 17 the CFD results are directly compared to the experiments because they are run with exactly the same boundary conditions. In the case of Fig. 18, although the non dimensional parameters are kept the same, the physical boundary conditions are not. For this reason a comparison between CFD and experiments for constant $T_{0_{in}}$ has been avoided.

It is interesting to notice how in this case the model is able to describe, at least qualitatively, the same trend seen in experimental data. Both the computations and the experiments show that an increase of the temperature ratio destabilizes the flow. Dif-

Copyright © 2018 by ASME

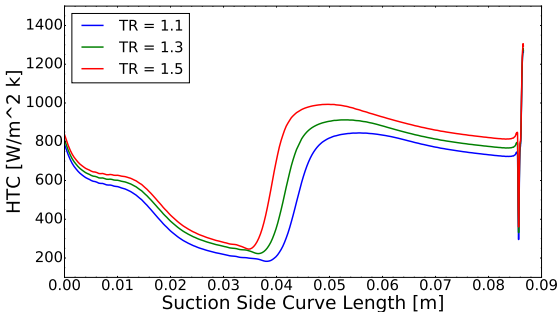

FIGURE 18: Blade HTC distribution obtained from the simulations at different TR obtained at constant $T_{0_{in}}$

ferently from what observed with the $\gamma - Re_\theta$ model, this same effect is predicted in both simulation campaign — at constant T_w and constant $T_{0_{in}}$ — though with different sensitivity. This illustrates how a locally based approach to transition modelling (rather than correlation based) should be favoured when thermal effects are of interest.

As done for the $\gamma - Re_\theta$ a deeper analysis of the flow evolution through the boundary layer traversing has been performed. The main results are discussed in the following paragraphs. Since the behaviour of the model has been observed to be very similar in both conditions, the results are summarized in a single section and only results obtained at constant $T_{0_{in}}$ are shown for the sake of brevity.

Velocity: Velocity profiles shown in Fig. 19 indicate that: in the fully laminar and turbulent part of the boundary layer the velocity profile does not feel a strong influence of the different temperature field. Differences can be observed in sections 3 and 4, this is due the fact that the case with higher temperature ratio has already reached transition while the blue one is still in a pre-transitional configuration, this generates two marginally different velocity profiles along the blade. The results for the case at constant T_w are analogous.

Kinematic viscosity: The results on the kinematic viscosity field are similar to what was seen for the $\gamma - Re_\theta$ transition model. From Fig. 20 the overall effect is a decrease of the kinematic viscosity with an increase of the TR. The same effect has been observed for constant T_w.

Turbulent variables: Figures 21 to 23 show the evolution of relevant turbulent variables under constant $T_{0_{in}}$ conditions.

From the analysis of the behaviour of k_l (Fig. 21), k (Fig. 22) and the turbulent kinetic energy transfer (Fig. 23) between these two, it is possible to understand how the model works. For both cases, the movement of the transition location upstream for the high TR case, causes an enhancement of the laminar kinetic energy in section 3 (pre-transitional location). The turbulent kinetic

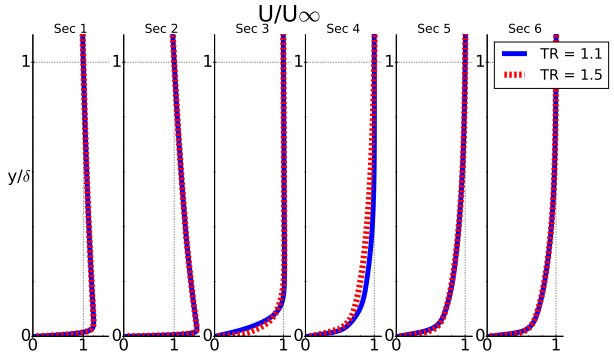

FIGURE 19: Distribution of velocity magnitude across the boundary layer traversing locations. $k - k_l - \omega$ model, constant $T_{0_{in}}$.

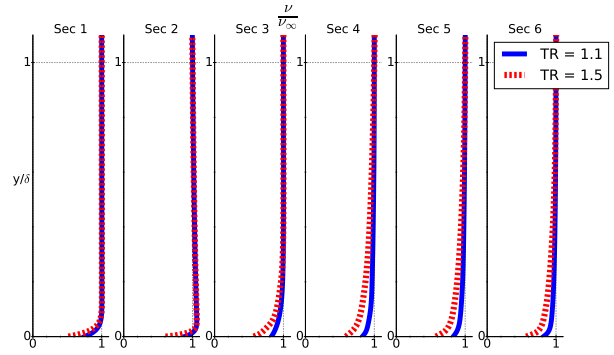

FIGURE 20: Distribution of kinematic viscosity across the boundary layer traversing locations. $k - k_l - \omega$ model, constant $T_{0_{in}}$.

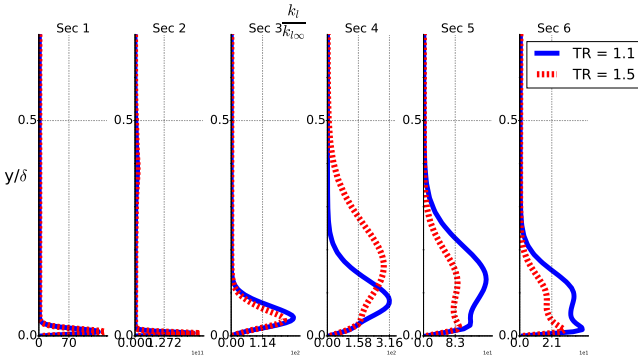

FIGURE 21: Distribution of laminar kinetic energy k_l across the boundary layer traversing locations. $k - k_l - \omega$ model, constant $T_{0_{in}}$.

Copyright © 2018 by ASME

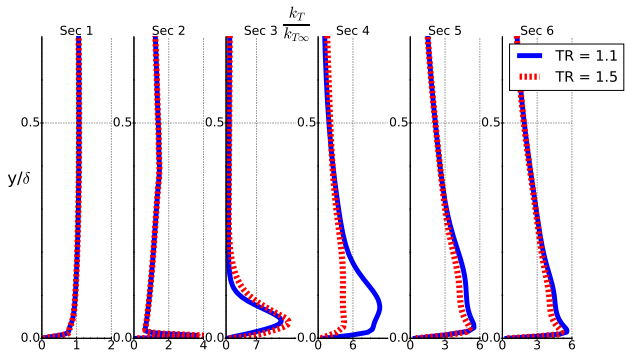

FIGURE 22: Distribution of turbulent kinetic energy k across the boundary layer traversing locations. $k-k_l-\omega$ model, constant $T_{0_{in}}$.

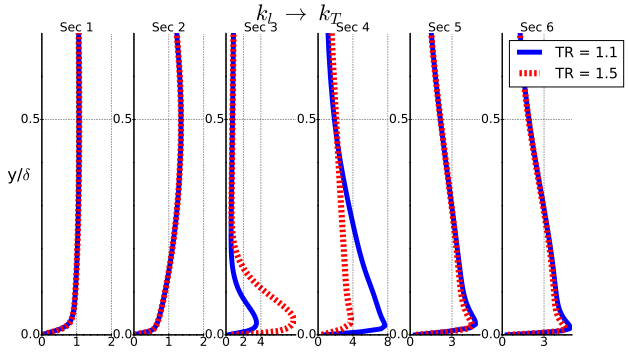

FIGURE 23: Distribution of turbulent energy transfer across the boundary layer traversing locations. $k-k_l-\omega$ model, constant $T_{0_{in}}$.

energy shows a complementary behaviour: increasing remarkably once the transition is triggered. The increase of turbulent kinetic energy after transition is due to the effect of wall TR on the ratio of transport of energy from the large scales to the smaller scales (Fig. 23). The high TR case shows a considerably higher distribution of the kinetic energy transfer term in section 3, corresponding to an anticipated transition.

6.5 $k-k_l-\omega$ concluding remarks

The behaviour of the $k-k_l-\omega$ model corresponds more closely to what the experimental results are suggesting. In the three tests cases with constant T_w the comparison between the experimental results and the computations shows that the trend of transition movement with TR is captured correctly, together with a reasonable accuracy on general heat transfer levels. Most importantly — and in a markedly different way than the $\gamma-Re_\theta$ model — the model gives the same predictions at both constant T_w and constant freestream conditions.

This behaviour could be due to the fact that the model does not rely on empirical correlations to trigger transition. The philosophy of the model is to track the evolution of the pre-transitional fluctuations (laminar kinetic energy); when they reach a certain value they activate a threshold function that triggers the transport of energy from the larger scales to the smaller ones. The threshold function is:

$$\phi_{BP} = max[\frac{k}{\nu\Omega} - C_{BPcrit}, 0] \tag{4}$$

We can see how the main variables that drive the value of ϕ_{BP} are the turbulent kinetic energy k, the vorticity Ω and the kinematic viscosity μ. It has been observed that, at least in the pre-transitional part of the boundary layer, the turbulent kinetic energy and the vorticity are very similar for the two temperature ratios. However the kinematic viscosity related to the freestream value shows a bigger decrease for the case at higher temperature ratio. It is reasonable to believe that the variation of the viscosity inside the boundary layer is the main cause of the variation of the threshold function leading to a destabilization of the flow.

The reasons of the good behaviour of this kind of model with respect to the previous one could be attributed to the fact that the relations used to trigger the transition are based on local parameters, accounting for the boundary layer history, instead of relying on empirical correlations based heavily on freestream conditions.

7 CONCLUSIONS

The main target of this work was to understand the capabilities of two well established transition models in describing the behaviour of a cooled boundary layer in a flow field characterized by non negligible compressibility effects.

The two transition models chosen are the $\gamma-Re_\theta$ [17] and the $k-k_l-\omega$ [2]. Numerical simulations have been performed and the results compared with the experimental results coming from a parallel experimental project.

In order to be able to extract the temperature effect on the transition of the boundary layer, both the experiments and the computations have been performed at constant exit Mach and Reynolds numbers. The experimental setup allowed to alter the wall to free-stream temperature ratio only by varying the free-stream conditions while keeping wall conditions constant. In numerical experiments the same temperature ratio was obtained in two ways: altering the free-stream conditions as well as altering the blade wall temperature (with constant free-stream).

This has been done to expose the different philosophies behind the two used models (correlation-based for the $\gamma-Re_\theta$ while $k-k_l-\omega$ is only based on local transport).

The correlation of the $\gamma-Re_\theta$ caused the model to give inconsistent results between the two scenarios. Given the formulation of the model, one possible explanation of this behaviour could be the fact that the value of the Re_θ is strongly influenced by the free-stream conditions and only marginally affected by the temperature of the wall.

Copyright © 2018 by ASME

Owing to its local formulation, the $k-k_l-\omega$ model showed similar effects of the temperature ratio, disregarding whether the same TR was obtained by altering the wall or the free-stream conditions. The model showed also a higher level of affinity with the experimental results, showing a destabilization of the boundary layer with cooling, though the magnitude of the transition point shifting was not correctly predicted.

The results of this work suggest that a local transport approach, not resorting to experimental correlations, should be favoured when trying to model the effect of TR on transition. This said even the $k-k_l-\omega$ transition model, that is only based on local transport, seems to fall short in correctly predicting the magnitude of TR on transition. A deeper understanding of the mechanism that influences transition through the TR should be sought through detailed aero-thermal measurements under bypass transition. As pointed out in the introduction to the present work, this is a field where very poor literature has been produced over the years. A solid knowledge, backed up by detailed experimental data, will provide the indications of how to improve current models to accurately capture the effects of TR.

References

[1] R. B. Langtry and F. R. Menter. Correlation-based transition modeling for unstructured parallelized computational fluid dynamics codes. *AIAA journal*, 47(12):2894–2906, 2009.

[2] D. Keith Walters and D. Cokljat. A three-equation eddy-viscosity model for Reynolds-averaged Navier Stokes simulations of transitional flow. *Journal of fluids engineering*, 130(12):121401, 2008.

[3] Robert Edward Mayle. The 1991 igti scholar lecture: The role of laminar-turbulent transition in gas turbine engines. *Journal of Turbomachinery*, 113(4):509–536, 1991.

[4] J.H. Horlock and J.D. Denton. A review of some early design practice using computational fluid dynamics and a current perspective. *Journal of Turbomachinery*, 127(1):5–13, 2005.

[5] Roberto Maffulli and Li He. Wall temperature effects on heat transfer coefficient for high-pressure turbines. *Journal of Propulsion and Power*, 30(4):1080–1090, 2014.

[6] Roberto Maffulli and Li He. Impact of wall temperature on heat transfer coefficient and aerodynamics for three-dimensional turbine blade passage. *Journal of Thermal Science and Engineering Applications*, 9(4):041002, 2017.

[7] S. Ozgen. Effect of heat transfer on stability and transition characteristics of boundary-layers. *International journal of heat and mass transfer*, 47(22):4697–4712, 2004.

[8] P. Schafer, J. Severin, and H. Herwig. The effect of heat transfer on the stability of laminar boundary layers. *International journal of heat and mass transfer*, 38(10):1855–1863, 1995.

[9] S. B. Harrison, D. J. Mee, and T. V. Jones. Experiment on the influence of heating on boundary layer transition in favourable pressure gradients. In *Proceedings Eurotherm Seminar*, 1991.

[10] O. Sharma. Momentum and thermal boundary layers on turbine airfoil suction surfaces. In *23rd Joint Propulsion Conference*, page 1918, 1987.

[11] K.H. Sohn, J.E. OBrien, and E. Reshotko. Some characteristics of bypass transition in a heated boundary layer. In *Turbulent Shear Flows 7*, pages 137–153. Springer, 1991.

[12] Tânia S. Cação Ferreira and Tony Arts. Influence of gas-to-wall temperature ratio on by-pass transition. ASME paper GT2017-36524.

[13] Daniel Arnal and Olivier Vermeersch. Compressibility effects on laminar-turbulent boundary layer transition. *International Journal of Engineering Systems Modelling and Simulation*, 3(1-2):26–35, 2011.

[14] L.H. Back, R.F. Cuffel, and P.F. Massier. Laminar, transition, and turbulent boundary-layer heat-transfer measurements with wall cooling in turbulent airflow through a tube. *Journal of Heat Transfer*, 91(4):477–487, 1969.

[15] Eli Reshotko and Anatoli Tumin. Role of transient growth in roughness-induced transition. *AIAA journal*, 42(4):766–770, 2004.

[16] RE Mayle and A Schulz. Heat transfer committee and turbomachinery committee best paper of 1996 award: The path to predicting bypass transition. *Journal of turbomachinery*, 119(3):405–411, 1997.

[17] Florian R. Menter, Robin Blair Langtry, S.R. Likki, Y.B. Suzen, P.G. Huang, and S. Völker. A correlation-based transition model using local variablespart i: model formulation. *Journal of turbomachinery*, 128(3):413–422, 2006.

[18] T. Arts, M. Lambert de Rouvroy, and C.H. Sieverding. Highly loaded transonic linear turbine guide vane cascade LS89. *Numerical Methods for flows in turbomachinery, von Karman Institute LS*, 6:22–26, 1989.

[19] T. Arts, L. De Rouvroit, and A.W. Rutherford. *Aero-thermal investigation of a highly loaded transonic linear turbine guide vane cascade - A test case for inviscid and viscous flow computations, VKI TN 174*. von Karman Institute for Fluid Dynamics, 1990.

[20] F. Fontaneto. *Aero-thermal performance of a film-cooled high pressure turbine blade / vane: a test case for numerical code validation*. PhD thesis, Universit degli studi di Bergamo, 2014.

[21] E.R.G. Eckert and R.M. Drake. *Analysis of heat and mass transfer*. Hemisphere Publishing, 1987.

[22] William Morrow Kays. *Convective heat and mass transfer*. Tata McGraw-Hill Education, 2012.

Copyright © 2018 by ASME